Soliton fiber laser mode locked with two types of film-based Bi_2Te_3 saturable absorbers

Dong Mao,[1] Biqiang Jiang,[1] Xuetao Gan,[1] Chaojie Ma,[1] Yu Chen,[2] Chujun Zhao,[2] Han Zhang,[2,3] Jianbang Zheng,[1] and Jianlin Zhao[1,*]

[1]*Key Laboratory of Space Applied Physics and Chemistry, Ministry of Education; and Shaanxi Key Laboratory of Optical Information Technology, School of Science, Northwestern Polytechnical University, Xi'an 710072, China*
[2]*SZU-NUS Collaborative Innovation Centre for Optoelectronic Science & Technology, College of Optoelectronic Engineering, Shenzhen University, Shenzhen 518060, China*
[3]*e-mail: hzhang@szu.edu.cn*
**Corresponding author: jlzhao@nwpu.edu.cn*

Received December 8, 2014; revised February 2, 2015; accepted February 16, 2015; posted February 18, 2015 (Doc. ID 229140); published March 26, 2015

We propose a low-threshold soliton fiber laser passively mode locked with two different types of film-like saturable absorbers, one of which is fabricated by mixing Bi_2Te_3 with de-ionized water, as well as polyvinyl alcohol (PVA), and then evaporating them in a Petri dish, and the other of which is prepared by directly dropping Bi_2Te_3 solution on the PVA film. Both Bi_2Te_3–PVA films exhibit outstanding features of low loss, high flexibility, and easy synthesis. By incorporating Bi_2Te_3–PVA films into fiber lasers, stable single-soliton emissions are obtained at a low pump power of 13 mW. Our results suggest that the Bi_2Te_3 can work as a promising mode locker for ultrafast lasers, while PVA is an excellent host for fabricating high-performance film-based saturable absorbers.

OCIS codes: (140.4050) Mode-locked lasers; (140.3510) Lasers, fiber; (160.4236) Nanomaterials; (190.7110) Ultrafast nonlinear optics.
http://dx.doi.org/10.1364/PRJ.3.000A43

1. INTRODUCTION

Ultrafast fiber lasers have attracted a great deal of research interest due to their widespread applications in the fields of fiber telecommunications, material processing, frequency combs, nonlinear microscopy [1–4], etc. In recent decades, various techniques, including *Q*-switching and active and passive mode locking, were proposed to produce ultrashort pulsed lasers. In active mode locking, an optical modulator is utilized to modify the phase or amplitude of lasers, which is inconvenient and increases the cost for practical applications [5]. For passively mode-locked fiber lasers, a saturable absorber (SA) is indispensable in shaping the pulse in the temporal domain [6]. One kind of SA is based on nonlinear and/or birefringent effects, such as the Kerr lens [7], nonlinear polarization rotation technique [8,9], and nonlinear optical loop mirror [10,11]. These devices exhibit features of a large damage threshold and broad operating wavelength range, while they are less stable and tend to be affected by environmental perturbations. The other kind of SA arises from the nonlinear absorption of materials, such as the semiconductor saturable absorber mirror (SESAM) [12–14], carbon nanotube [15–17], graphene [18,19], MoS_2 [20–22], and WS_2 [23]. Among them, the SESAM and carbon nanotube have large modulation depths and are designed to operate at certain wavelengths. As a result of the unique zero bandgap, a graphene-based SA exhibits a broadband response and has been used in a mode-locked fiber laser operating at 1.06, 1.55, and 2 μm, respectively [24].

Currently, motivated by graphene-like two-dimensional materials, topological insulators (TIs), a new state of quantum matter with an insulating bulky gap and gapless edge or surface states, have been investigated in depth in condensed-matter physics and laser photonics [25–27]. A TI has a single Dirac cone on the surface around the Γ point and a small bandgap of 0.2–0.3 eV in the bulk. For a gap of 0.3 eV, a photon can excite an electron from the valence band to the conduction band when the light wavelength is shorter than 4.1 μm [28]. As a result, TI may work as an ultrabroadband nonlinear element manipulating the light waves. Bernard *et al.* first demonstrated that Bi_2Te_3 exhibited SA behavior at the telecommunication band [29]. Zhao *et al.* experimentally realized passive mode locking in a soliton fiber laser by dropping a Bi_2Te_3 solution onto a quartz plate [30]. Recently, Luo *et al.* achieved a 2 GHz harmonic mode-locked fiber laser using a microfiber-based Bi_2Te_3 SA [31]. Moreover, Lin *et al.* [32], Jung *et al.* [33], and Lee *et al.* [34] demonstrated that Bi_2Te_3 coated on the end-face of fiber, mechanically exfoliated Bi_2Te_3, and bulk-structured Bi_2Te_3 can act as effective SAs in fiber lasers. Sotor *et al.* [35] and Liu *et al.* [36] proposed a mode-locked erbium-doped fiber (EDF) laser using mechanically exfoliated Sb_2Te_3 and polyvinyl alcohol (PVA)-based Sb_2Te_3 SAs. These proposed SAs demonstrate an interesting step forward in the fields of TI-based ultrafast optics. However, compared with other methods, the film-based SA would be more favorable due to its superior attributes of low cost, flexibility, and controllability.

In this paper, we propose two methods to fabricate film-based SAs by combining Bi_2Te_3 and PVA. One type of film is formed by homogeneously mixing Bi_2Te_3 with de-ionized water, as well as PVA, and then evaporating them in a Petri

dish. The other type of film is prepared by directly dropping the Bi_2Te_3 solution on the PVA film. By using two types of SAs, conventional solitons operating at the telecommunication band are achieved separately in the fiber laser at a low pump power of 13 mW. The experimental results show that both Bi_2Te_3–PVA films can work as flexible, broadband, and cost-effective mode lockers that can find important applications in ultrafast optics.

2. PREPARATION AND CHARACTERIZATION OF A Bi_2Te_3–PVA-BASED SA

The Bi_2Te_3 nanosheets were synthesized by the hydrothermal intercalation/exfoliation approach [30]. Based on previous reports [37], the recovery time of interband scattering from the bulk conduction band is about 0.5 ps, while the relaxation time for the Dirac cone nonequilibrium electrons to recover a Fermi–Dirac distribution of the surface states is over 10 ps. Figure 1(a) shows the scanning electron microscopy image of Bi_2Te_3 nanosheets deposited on a quartz plate, in which well-exfoliated hexagonal nanosheets with a size of 0.5–1 μm can be seen clearly. The as-prepared Bi_2Te_3 nanosheets were dispersed in isopropyl alcohol with a concentration of ~0.1 mg/mL, as shown in Fig. 1(b). In our experiment, two different methods were used to fabricate the film-based SAs. The first method is as follows. The obtained Bi_2Te_3 solutions were diluted in de-ionized water at a volume ratio of 1:4 and ultrasonicated for 1 h using an ultrasonic cleaner. Then, 5 wt. % aqueous PVA solution and the Bi_2Te_3 solution were mixed at a volume ratio of 1:2 by a magnetic stirrer for 5 h. The final mixture was dropped on a Petri dish. Slow evaporation under ambient temperature and pressure resulted in a thin Bi_2Te_3–PVA composite film, as shown in the top of Fig. 1(c). Here, the concentration of Bi_2Te_3 can be precisely controlled and excessive agglomeration of Bi_2Te_3 can be eliminated to avoid unwanted insertion loss. The second method is much simpler and is different from that in previous reports [36]. The amounts of the PVA and Bi_2Te_3 solutions are the same as in the first method. The PVA film was fabricated by dropping the PVA solution on a Petri dish. After evaporation, the Bi_2Te_3 nanosheets in isopropyl alcohol were directly dropped on both sides of the PVA film and were evaporated for tens of minutes, as shown in the bottom of Fig. 1(c). Because the SA is formed by directly dropping the solution on film, the fabrication procedure, time, and cost are significantly reduced. However, the concentration and agglomeration of the second SA cannot be precisely controlled, which will further affect the mode-locking performance. This fabrication

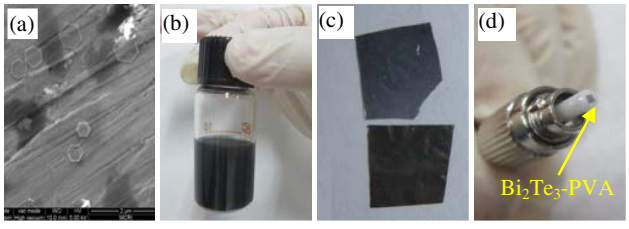

Fig. 1. (a) Scanning electron microscopy image of Bi_2Te_3 nanosheets, (b) Bi_2Te_3 isopropyl alcohol solutions, (c) Bi_2Te_3–PVA film, where the top and bottom films are prepared by the first and second methods, respectively, and (d) Bi_2Te_3–PVA film attached to the facet of a fiber connector.

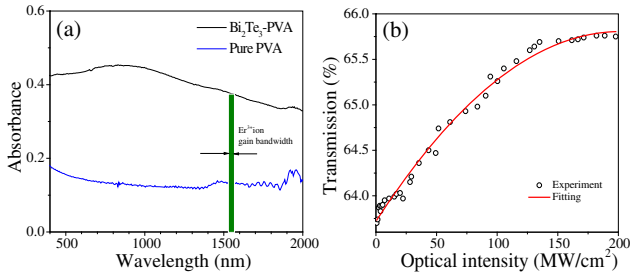

Fig. 2. (a) Absorption spectra of Bi_2Te_3–PVA and pure PVA films, where the vertical olive line illustrates the spectral gain region of the EDF, (b) nonlinear absorption characterization of the Bi_2Te_3–PVA SA. The solid curve is fitted from the experimental data (circle symbols).

method may also apply to graphene, nanotube, and MoS_2 solutions. Figure 1(d) shows a photograph of Bi_2Te_3–PVA film that is coated on the facet of the fiber connector.

Figure 2(a) shows the linear absorption spectrum of the Bi_2Te_3–PVA film in comparison with pure PVA, which is measured by a spectrometer (Hitachi UV4100). It is demonstrated that the Bi_2Te_3 exhibits a relatively broad transmission from the visible to near-IR wave band, indicating that Bi_2Te_3 could be another broadband optical material manipulating light waves. The nonlinear absorption of the Bi_2Te_3 SA was experimentally measured by a power-dependent transmission technique based on a balanced twin-detector measurement system, which was elaborated in Ref. [31]. The illumination pulse was delivered by a homemade passively mode-locked fiber laser (repetition rate: 20 MHz, pulse duration: 1.8 ps, central wavelength: 1560 nm). As shown in Fig. 2(b), the modulation depth is about 2% and the nonsaturable loss is about 34% after fitting the measured data. The saturable optical intensity and saturation fluence of the SA at 1560 nm are about 180 MW/cm^2 and 3.3 mW, respectively. In addition, we measured the nonlinear proprieties of the same SA several times and found that the saturable absorption parameters were almost identical, indicating that the device was beyond the damage threshold during the test procedures.

3. EXPERIMENTAL SETUP AND RESULTS

Figure 3 shows the experimental setup of the fiber laser. The mode locker is assembled by sandwiching the Bi_2Te_3–PVA film between two fiber ferrules, as shown in the inset. The laser resonator consists of 3 m EDF, a polarization-insensitive

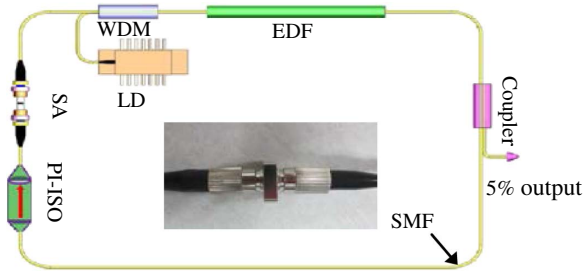

Fig. 3. Experimental setup of the fiber laser with Bi_2Te_3 as a mode locker. LD, laser diode; WDM, wavelength division multiplexer; PI-ISO, polarization insensitive isolator. The SA is achieved by sandwiching the Bi_2Te_3–PVA film between two fiber ferrules, as demonstrated in the inset.

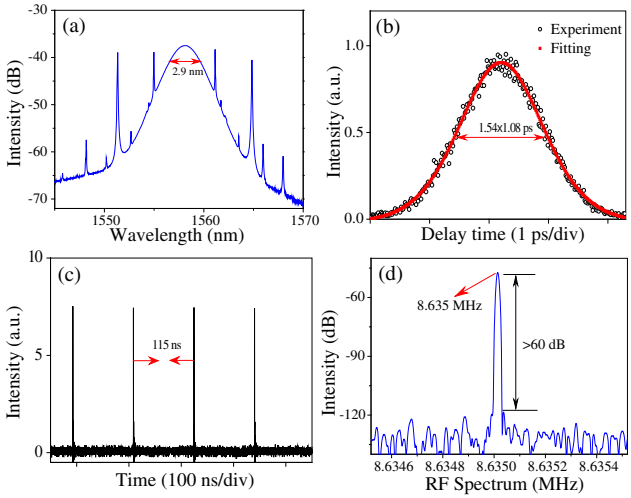

Fig. 4. (a) Spectrum, (b) autocorrelation trace, (c) oscilloscope trace, and (d) RF spectrum of the pulse. The SA is fabricated by dispersing the Bi_2Te_3 into PVA (first method).

isolator, and a SA. The fiber laser is pumped by a 975 nm laser diode through a wavelength division multiplexer coupler. The 5% port of an optical coupler provides the laser output. All of the other fibers are standard single-mode fiber (SMF) with a total length of 20.8 m. The dispersion parameters D at 1550 nm for EDF and SMF are −16 and 17 ps/(nm · km), respectively. The net cavity dispersion β^2 is calculated as −0.39 ps^2.

Continuous wave emission was achieved at an incident pump power of 6 mW using Bi_2Te_3–PVA film fabricated by the first method (Bi_2Te_3 mixed with PVA). Self-starting soliton mode locking was observed at a pump power of 30 mW. In this case, the fiber laser operated at the multisoliton state and the output power was about 0.4 mW. Decreasing the pump power to 13 mW, stable single-soliton mode locking was realized in the fiber laser with an output power about 0.14 mW. At a pump power of 19 mW, a single pulse was split into dual pulses with an output power of 0.25 mW. Figure 4(a) shows the output spectrum, which exhibits symmetrically distributed Kelly sidebands on both sides. The small spectral sidebands may arise from the inherent four-wave mixing of the vector soliton [38], confirming that the as-fabricated passive mode locker is polarization insensitive. The central wavelength and 3 dB spectral bandwidth are measured to be 1557 and 2.9 nm, respectively. We also found that the laser wavelength was shifted toward longer wavelengths by increasing the pump power, which may be attributed to the joint contribution from the Raman effect and pump-dependent gain effect [39,40].

Figure 4(b) shows the autocorrelation trace of the output soliton measured with a high-sensitivity autocorrelator. The FWHM of the autocorrelation trace is about 1.59 ps, and the pulse duration is found to be 1.08 ps by using the $sech^2$ fitting. The corresponding time bandwidth product (TBP) is calculated as 0.39, indicating that the soliton has little chirp, which may arise from the nonlinear phase shift accumulated during amplification. As shown in Fig. 4(c), the separation between adjacent pulses is about 115 ns, which is equal to the cavity round-trip time. Figure 4(d) shows the RF spectrum at a span of 1 kHz and resolution of 9.1 Hz. The fundamental repetition rate is given as 8.635 MHz, which coincides

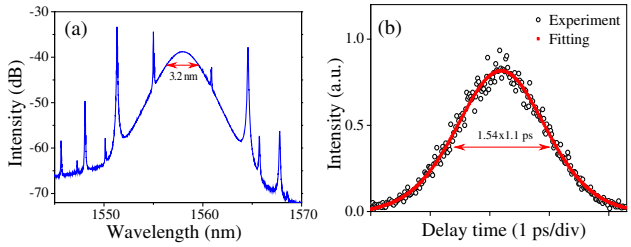

Fig. 5. (a) Spectrum and (b) autocorrelation trace of the pulse. Herein, the SA is formed by directly dropping the Bi_2Te_3 solution on the PVA film (second method).

with the temporal separation of 115 ps. The signal-to-noise ratio is higher than 60 dB, indicating its good mode-locking stability.

Utilizing the Bi_2Te_3–PVA film fabricated by the second method (Bi_2Te_3 solution dropped on PVA film), stable soliton mode locking can be also achieved in the same fiber laser. The oscilloscope trace and RF spectrum are similar to Figs. 4(c) and 4(d) and are omitted for conciseness. Figures 5(a) and 5(b) show the spectrum and autocorrelation trace of the pulse at the same pump power of 13 mW, respectively. The output power is measured as 0.11 mW, slightly less than in the first case, which may be attributed to a larger insertion loss of the second SA. Here, the 3 dB spectral width and pulse duration are given as 3.2 and 1.1 ps, which gives a TBP of 0.44. The TBP difference of the two operations may be attributed to the change of SA or external conditions, such as fiber bends and loss.

The experimental results show that the damage thresholds for the first and second SAs are about 240 and 180 mW, respectively. Fiber lasers mode locked with Bi_2Te_3–PVA SAs can stably operate at the same state for tens of hours as long as the pump power is kept unchanged, and they can withstand slight mechanical perturbation and temperature variations. To verify whether the soliton formation is caused by only the saturable absorption of the Bi_2Te_3, we have purposely removed or replaced the Bi_2Te_3–PVA film with pure PVA film from a laser cavity. No mode locking was observed in either case, despite the fact that the pump power was changed from zero to the maximum and the fiber was bent and twisted over a large range. Based on the aforementioned results, we conclude that Bi_2Te_3 plays a key role in realizing passive mode locking in the fiber laser.

4. CONCLUSIONS

We have proposed two different methods of fabricating a film-based SA by combining Bi_2Te_3 and PVA. One of the films is formed by homogeneously mixing Bi_2Te_3, de-ionized water, and PVA, and then evaporating them in a Petri dish. The other film is prepared by directly dropping the Bi_2Te_3 solution on the PVA film. The two types of SAs exhibit the features of broadband transmission, low cost, and ease of fabrication. By inserting the Bi_2Te_3–PVA films inside the laser cavity, a single soliton can be obtained at a pump power of 13 mW, which is quite low in mode-locked fiber lasers. Our results suggest that the PVA is an excellent host for fabricating a high-performance SA, and the Bi_2Te_3 can be further developed as a useful passive mode-locking element.

ACKNOWLEDGMENTS

This work was supported by the Fundamental Research Funds for the Central Universities (Grant Nos. 3102014JCQ01101, 3102014JCQ01099, and 3102014JCQ01085), the 973 Program (Grant No. 2012CB921900), and the National Natural Science Foundation of China (Grant Nos. 61405161, 11404263, and 61377035).

References

1. M. E. Fermann and I. Hartl, "Ultrafast fibre lasers," Nat. Photonics **7**, 868–874 (2013).
2. C. Xu and F. W. Wise, "Recent advances in fibre lasers for nonlinear microscopy," Nat. Photonics **7**, 875–882 (2013).
3. D. Mao, X. Liu, Z. Sun, H. Lu, D. Han, G. X. Wang, and F. Wang, "Flexible high-repetition-rate ultrafast fiber laser," Sci. Rep. **3**, 3233 (2013).
4. S. Smirnov, S. Kobtsev, and S. Kukarin, "Efficiency of non-linear frequency conversion of double-scale pico-femtosecond pulses of passively mode-locked fiber laser," Opt. Express **22**, 1058–1064 (2014).
5. K. Yin, B. Zhang, W. Yang, S. Chen, and J. Hou, "Flexible picosecond thulium-doped fiber laser using the active mode-locking technique," Opt. Lett. **39**, 4259–4262 (2014).
6. H. A. Haus, "Mode-locking of lasers," IEEE J. Sel. Top. Quantum Electron. **6**, 1173–1185 (2000).
7. T. Brabec, C. Spielmann, P. Curley, and F. Krausz, "Kerr lens mode locking," Opt. Lett. **17**, 1292–1294 (1992).
8. Z. C. Luo, A. P. Luo, W. C. Xu, C. X. Song, and Y. X. Gao, "Sideband controllable soliton all-fiber ring laser passively mode-locked by nonlinear polarization rotation," Laser Phys. Lett. **6**, 582–585 (2009).
9. D. Mao, X. M. Liu, L. R. Wang, X. H. Hu, and H. Lu, "Partially polarized wave-breaking-free dissipative soliton with superbroad spectrum in a mode-locked fiber laser," Laser Phys. Lett. **8**, 134–138 (2011).
10. L. M. Zhao, A. C. Bartnik, Q. Q. Tai, and F. W. Wise, "Generation of 8 nJ pulses from a dissipative-soliton fiber laser with a nonlinear optical loop mirror," Opt. Lett. **38**, 1942–1944 (2013).
11. L. Yun, X. Liu, and D. Mao, "Observation of dual-wavelength dissipative solitons in a figure-eight erbium-doped fiber laser," Opt. Express **20**, 20992–20997 (2012).
12. D. Y. Tang, H. Zhang, L. M. Zhao, and X. Wu, "Observation of high-order polarization-locked vector solitons in a fiber laser," Phys. Rev. Lett. **101**, 153904 (2008).
13. U. Keller, "Recent developments in compact ultrafast lasers," Nature **424**, 831–838 (2003).
14. D. Mao, X. M. Liu, and H. Lu, "Observation of pulse trapping in a near-zero dispersion regime," Opt. Lett. **37**, 2619–2621 (2012).
15. S. Y. Set, H. Yaguchi, Y. Tanaka, and M. Jablonski, "Ultrafast fiber pulsed lasers incorporating carbon nanotubes," IEEE J. Sel. Top. Quantum Electron. **10**, 137–146 (2004).
16. X. Liu, D. Han, Z. Sun, C. Zeng, H. Lu, D. Mao, Y. Cui, and F. Wang, "Versatile multi-wavelength ultrafast fiber laser mode-locked by carbon nanotubes," Sci. Rep. **3**, 2718 (2013).
17. F. Wang, A. Rozhin, V. Scardaci, Z. Sun, F. Hennrich, I. White, W. Milne, and A. Ferrari, "Wideband-tuneable, nanotube mode-locked, fibre laser," Nat. Nanotechnol. **3**, 738–742 (2008).
18. H. Zhang, Q. Bao, D. Tang, L. Zhao, and K. Loh, "Large energy soliton erbium-doped fiber laser with a graphene-polymer composite mode locker," Appl. Phys. Lett. **95**, 141103 (2009).
19. Z. Sun, T. Hasan, F. Torrisi, D. Popa, G. Privitera, F. Wang, F. Bonaccorso, D. Basko, and A. Ferrari, "Graphene mode-locked ultrafast laser," ACS Nano **4**, 803–810 (2010).
20. H. Zhang, S. B. Lu, J. Zheng, J. Du, S. C. Wen, D. Y. Tang, and K. P. Loh, "Molybdenum disulfide MoS_2 as a broadband saturable absorber for ultra-fast photonics," Opt. Express **22**, 7249–7260 (2014).
21. J. Du, Q. Wang, G. Jiang, C. Xu, C. Zhao, Y. Xiang, Y. Chen, S. Wen, and H. Zhang, "Ytterbium-doped fiber laser passively mode locked by few-layer molybdenum disulfide (MoS_2) saturable absorber functioned with evanescent field interaction," Sci. Rep. **4**, 6346 (2014).
22. H. Xia, H. Li, C. Lan, C. Li, X. Zhang, S. Zhang, and Y. Liu, "Ultrafast erbium-doped fiber laser mode-locked by a CVD-grown molybdenum disulfide (MoS_2) saturable absorber," Opt. Express **22**, 17341–17348 (2014).
23. D. Mao, Y. Wang, C. Ma, L. Han, B. Jiang, X. Gan, S. Hua, W. Zhang, T. Mei, and J. Zhao, "WS_2 mode-locked ultrafast fiber laser," Sci. Rep. **5**, 7965 (2015).
24. X. Li, Y. Tang, Z. Yan, Y. Wang, B. Meng, G. Liang, H. Sun, X. Yu, Y. Zhang, X. Cheng, and Q. Wang, "Broadband saturable absorption of graphene oxide thin film and its application in pulsed fiber lasers," IEEE J. Sel. Top. Quantum Electron. **20**, 1101107 (2014).
25. M. Hasan and C. Kane, "Colloquium: topological insulators," Rev. Mod. Phys. **82**, 3045–3067 (2010).
26. A. B. Khanikaev, S. H. Mousavi, W. K. Tse, M. Kargarian, A. H. MacDonald, and G. Shvets, "Photonic topological insulators," Nat. Mater. **12**, 233–239 (2013).
27. H. Zhang, C. X. Liu, X. L. Qi, X. Dai, Z. Fang, and S. C. Zhang, "Topological insulators in Bi_2Se_3, Bi_2Te_3 and Sb_2Te_3 with a single Dirac cone on the surface," Nat. Phys. **5**, 438–442 (2009).
28. H. Yu, H. Zhang, Y. Wang, C. Zhao, B. Wang, S. Wen, H. Zhang, and J. Wang, "Topological insulator as an optical modulator for pulsed solid-state lasers," Laser Photon. Rev. **7**, 77–83 (2013).
29. F. Bernard, H. Zhang, S. P. Gorza, and P. Emplit, "Towards mode-locked fiber laser using topological insulators," in *Advanced Photonics Congress*, OSA Technical Digest (online) (Optical Society of America, 2012), paper NTh1A.5.
30. C. Zhao, H. Zhang, X. Qi, Y. Chen, Z. Wang, S. Wen, and D. Tang, "Ultra-short pulse generation by a topological insulator based saturable absorber," Appl. Phys. Lett. **101**, 211106 (2012).
31. Z. C. Luo, M. Liu, H. Liu, X. W. Zheng, A. P. Luo, C. J. Zhao, H. Zhang, S. C. Wen, and W. C. Xu, "2 GHz passively harmonic mode-locked fiber laser by a microfiber-based topological insulator saturable absorber," Opt. Lett. **38**, 5212–5215 (2013).
32. Y. H. Lin, C. Y. Yang, S. F. Lin, W. H. Tseng, Q. Bao, C. I. Wu, and G. R. Lin, "Soliton compression of the erbium-doped fiber laser weakly started mode-locking by nanoscale p-type Bi_2Te_3 topological insulator particles," Laser Phys. Lett. **11**, 055107 (2014).
33. M. Jung, J. Lee, J. Koo, J. Park, Y.-W. Song, K. Lee, S. Lee, and J. H. Lee, "A femtosecond pulse fiber laser at 1935 nm using a bulk-structured Bi_2Te_3 topological insulator," Opt. Express **22**, 7865–7874 (2014).
34. J. Lee, J. Koo, Y. M. Jhon, and J. H. Lee, "A femtosecond pulse erbium fiber laser incorporating a saturable absorber based on bulk-structured Bi_2Te_3 topological insulator," Opt. Express **22**, 6165–6173 (2014).
35. J. Sotor, G. Sobon, W. Macherzynski, P. Paletko, K. Grodecki, and K. M. Abramski, "Mode-locking in Er-doped fiber laser based on mechanically exfoliated Sb_2Te_3 saturable absorber," Opt. Mater. Express **4**, 1–6 (2014).
36. H. Liu, X. W. Zheng, M. Liu, N. Zhao, A. P. Luo, Z. C. Luo, W. C. Xu, H. Zhang, C. J. Zhao, and S. C. Wen, "Femtosecond pulse generation from a topological insulator mode-locked fiber laser," Opt. Express **22**, 6868–6873 (2014).
37. M. Hajlaoui, E. Papalazarou, J. Mauchain, G. Lantz, N. Moisan, D. Boschetto, Z. Jiang, I. Miotkowski, Y. P. Chen, A. Taleb-Ibrahimi, L. Perfetti, and M. Marsi, "Ultrafast surface carrier dynamics in the topological insulator Bi_2Te_3," Nano Lett. **12**, 3532–3536 (2012).
38. H. Zhang, D. Y. Tang, L. M. Zhao, and N. Xiang, "Coherent energy exchange between components of a vector soliton in fiber lasers," Opt. Express **16**, 12618–12623 (2008).
39. J. P. Gordon, "Theory of the soliton self-frequency shift," Opt. Lett. **11**, 662–664 (1986).
40. D. Mao and H. Lu, "Formation and evolution of passively mode-locked fiber soliton lasers operating in a dual-wavelength regime," J. Opt. Soc. Am. B **29**, 2819–2826 (2012).